www.sciencemag.org/cgi/content/full/1172278/DC1

Supporting Online Material for

Fluorescent False Neurotransmitters Visualize Dopamine Release from Individual Presynaptic Terminals

Niko G. Gubernator, Hui Zhang, Roland G. W. Staal, Eugene V. Mosharov, Daniela Pereira, Minerva Yue, Vojtech Balsanek, Paul A. Vadola, Bipasha Mukherjee, Robert H. Edwards, David Sulzer,* Dalibor Sames*

*To whom correspondence should be addressed. E-mail: ds43@columbia.edu (D. Sulzer); sames@chem.columbia.edu (D. Sames)

Published 7 May 2009 on *Science* Express
DOI: 10.1126/science.1172278

This PDF file includes:

Other Supporting Online Material for this manuscript includes the following:
(available at www.sciencemag.org/cgi/content/full/1172278/DC1)

Supporting Online Material For

Fluorescent False Neurotransmitters Visualize Dopamine Release From Individual Presynaptic Terminals

Niko G. Gubernator,[1,2*] Hui Zhang,[3,4*] Roland G. W. Staal,[3] Eugene V. Mosharov,[3] Daniela Pereira,[3] Minerva Yue,[3] Vojtech Balsanek,[1] Paul A. Vadola,[1] Bipasha Mukherjee,[6] Robert H. Edwards,[6] David Sulzer,[3,4,5#] Dalibor Sames[1#]

[*] These authors contributed equally to this work.

[#] To whom correspondence should be addressed. E-mail: ds43@columbia.edu, sames@chem.columbia.edu.

This PDF includes:

I. MATERIALS AND METHODS

1. Design Criteria for Fluorescent False Neurotransmitters

The chemical design of the novel probes loosely mimics the overall topology and physical properties of monoamine neurotransmitters. Specifically, the aminoethyl group was conserved while the aromatic system was expanded to engineer the desired fluorescent properties. In addition to fluorescence properties, it is paramount that the candidate compounds are mildly basic to provide the driving force for accumulation in the vesicles and sufficiently polar to disfavor passive transport to other acidic compartments such as lysosomes and acidic endosomes. Following these design guidelines, we developed compound FFN511.

2. Structural characterization of FFN511 (8-(2-Amino-ethyl)-2,3,5,6-tetrahydro-1*H*,4*H*-11-oxa-3a-aza-benzo[*de*]anthracen-10-one)

NMR 1H (300 MHz, CDCl3) δ ppm:

7.00 (s, 1H); 5.90 (s, 1H); 3.24 (m, 4H); 3.04 (m, 2H); 2.88 (t, 2H, J=6.5 Hz); 2.78 (m, 4H); 1.97 (m, 4H); 1.50 (bs, 2H).

NMR 13C (75 MHz, CDCl3) δ ppm:

162.4; 154.1; 151.4; 145.8; 121.4; 118.0; 107.9; 107.7; 107.0; 49.9; 49.5; 41.2; 35.7; 27.7; 21.5; 20.6; 20.5.

IR (NaCl, cm-1) 2939; 2845; 1702; 1612; 1553; 1519; 1428; 1378; 1312; 1182; 729.

LRMS (APCI+): 285 (C17H21N2O2, M+H).

3. FFN511 Photophysical Properties

Fluorescence measurements were acquired on a Jobin Yvon Fluorolog fluorescence spectrofluorometer (slits 3, HV 750) in 100 mM sodium phosphate pH 7 buffer or chloroform solution (Fig. S1). Measurements in striatal slice were visualized using a Zeiss LSM 510 NLO multiphoton laser scanning microscope with a Titanium-sapphire laser (excitation 760 nm/emission 480-520 nm) equipped with a 63 X 0.9 NA water immersion ultraviolet objective (Zeiss). In pH7 buffer the λem (max) is 501 nm, λex (max) is 406 nm. In chloroform the λem (max) is 447 nm, λex (max) is 391 nm while in slice the λem (max) is ~475 nm.

4. Uptake into primary adrenal chromaffin cells

Primary adrenal chromaffin cells. The cultures were prepared as previously described *(1)*. Briefly, adrenal glands from 3-6-month-old mice were dissected in ice-cold Hank's balanced salt saline (HBSS). The capsule and cortex of adrenal glands were removed and the remaining medullae cut in two pieces. After several washes with HBSS, the tissue was incubated with Ca^{2+}-free collagenase IA (250 units/ml, Worthington) in HBSS for 30 min at 30^{o}C with stirring. The digested tissue was rinsed three times and triturated gently in HBSS containing 1% heat-inactivated bovine serum albumin and 0.02% DNAse I. Dissociated cells were collected at 1000 x g for 2 min and resuspended in a culture medium comprised of DMEM, 10% fetal bovine serum, 2 mM glutamine, 50 units/ml penicillin, and 50 µg/ml streptomycin. The cell suspension (100 µl) was plated onto poly-D-lysine and laminin coated 1 cm^2 glass wells in 50 mm dishes and, after 1-2 hrs, the dishes were flooded with the culture medium. Cells were maintained in a 7% CO_2

incubator at 37^{o}C. All measurements were conducted between days 2-4 post-plating. The saline for cell incubation at room temperature contained 10 mM HEPES-NaOH (pH 7.2), 128 mM NaCl, 2 mM KCl, 2 mM $MgCl_2$, 1.2 mM $CaCl_2$, 1 mM NaH_2PO_4, 10 mM glucose.

Drugs and Reagents. The reversible VMAT inhibitor 2-hydroxy-2-ethyl-3-isobutyl-9,10-dimethoxy-1,2,3,4,6,7-hexahydrobenzo[a]quinolizin hydrochloride (Ro 4-1284) was a gift from Hoffman-La Roche (Nutley, NJ). Ro 4-1284 is a TBZ analogue distinguishable only by the pharmacokinetics and solubility from TBZ. All other compounds were obtained from Fisher Scientific (Springfield, NJ) or Sigma Chemical Co. (St. Louis, MO).

Uptake and Inhibition Studies. For experiments with chloroquine, 350 nM FFN511 was added to cell cultures at room temperature. Time lapse microscopy of FFN511 fluorescence intensity of chromaffin cells was measured at 10 minute intervals. Upon visual inspection, only healthy chromaffin cells (e.g. circular, unbroken etc.) were selected. The vitality of cells was confirmed by the presence of normal quantal catecholamine secretion and was established before each labeling study by amperometry. FFN511 uptake rates varied widely between cells (from 4 F. arb. units/min to 30 F. arb. units/min) and one or two cells were analyzed per assay. Uptake of FFN511 was displayed as average mean intracellular fluorescence subtracting fluorescent signal from media nearby. Experiments were performed on an Axiovert 135 TV microscope and analyzed by Axiovision 4.6 software.

Amperometry. Solutions used for amperometric recordings were as follows. The bath saline (pH 7.4) contained (in mM): 128 NaCl, 2 KCl, 1 NaH_2PO_4, 2 $MgCl_2$, 1.2 $CaCl_2$, 10

glucose, 10 HEPES-KOH. Secretagogue solution was identical with the exception of 90 NaCl and 40 KCl. Secretagogue was applied by local perfusion through a pressurized glass micropipette (Picospritzer, General Valve Co., Fairfield, NJ) for 5 sec at ~10 μm from the cell. A 5 μm diameter carbon fiber electrode held at +700 mV was pressed against the cell surface and catecholamine oxidation was monitored as amperometric current spikes. The current was filtered using a 4-pole 5 kHz Bessel filter built into an Axopatch 200B amplifier (Axon Instruments, Foster City, CA) and sampled at 25 kHz (ITC-18, Instrutech, Great Neck, NY). After secretagogue application, the amperometric current was recorded for 60 sec and the data were analyzed using a locally written routine in IGOR Pro (WaveMetrics, Lake Oswego, OR) *(2)*. The current was digitally filtered using a low-pass binomial 600 Hz filter and the root mean square of the noise (RMS noise) on the first derivative of the current (dI/dt) was measured in a segment of the trace that did not contain spikes. dI/dt was then used to detect amperometric events that were 4.5-fold larger than the RMS noise. To improve the quality of spike detection, the current was additionally filtered using low-pass binomial 150 Hz filter before taking dI/dt. For each amperometric spike, the following shape characteristics were determined: quantal size (Q, pC), amplitude (I_{max}, pA), duration at half-height ($t_{1/2}$, ms), rise-time between 25% and 75% of Imax excluding the pre-spike foot (t_{rise}, ms), and the incline of the rising phase (slope, pA/ms). The falling phase of a spike was characterized by two time constants ($\tau 1$ and $\tau 2$, ms) of the double-exponential fit of the current between 25% of I_{max} and spike's end. The number of catecholamine molecules released from individual vesicles (QN) was calculated as $QN = Q/(n\Delta F)$, where F = 96,485 C/mole is Faraday's constant and n = 2 is the number of electrons donated by each catecholamine molecule

(3). Spikes with I_{max} smaller than 3 pA and traces with fewer than 10 amperometric spikes were excluded from the analysis (Fig. S3).

5. FFN511's VMAT2 IC_{50} value

To measure FFN511's affinity for VMAT2, we assayed its ability to inhibit uptake of ^{3}H-serotonin by membranes from HEK cells stably expressing VMAT2 *(4)*. Uptake by 50 µg extract from at least two different membrane preparations was carried out in triplicate using 2 mM ATP, 20 nM 30 Ci/mmol serotonin and varying concentrations of FFN511 for 2 minutes at 29^{o}C.

6. Total internal reflection fluorescence microscopy (TIRFM)

To investigate the ability of FFN511-labeled vesicles to undergo stimulation-dependent exocytosis, we employed live-cell imaging with evanescent field microscopy. Fluorescence was excited in a narrow 70-120 nm thick layer of cytosol immediately adjacent to the coverslip with a 488 nm laser beam to produce total internal reflection (TIR) at the glass/cell interface. TIRFM was performed on a Nikon TE2000 equipped with a 60X PlanApo N.A.1.45 objective. Images were acquired using a cooled CCD (ORCA I, C4742-95, Hamamatsu) controlled by MetaMorph software. Cells were treated with 7 µM FFN511 for 10 min at 37^{o}C and rinsed twice. 300 images were taken from each studied cell at a rate of 2 frames per second (2.5 min total). At 60 sec, a 60 sec-long puff of 90 mM KCl was applied at ~10 µm from the cell through a pressurized glass micropipette (Picospritzer, General Valve Co., Fairfield, NJ). Detailed analysis of the kinetics of vesicle disappearance revealed that at the image acquisition rate of our

measurements (2 Hz), the fluorescence signal from a fusing vesicle typically reached the level of background within one frame, although similar to acridine orange studies *(5)*, sometimes a diffuse 'cloud' of fluorescence was visible due to diffusion from the vesicle to the media (Fig. S4), indicating exocytotic release.

7. FFN511 in Striatal Slices

Slice preparation. Two- to four-month old male C57BL/6 mice were obtained from The Jackson Laboratory (Bar Harbor, ME). All animal protocols were approved by the IACUC of Columbia University. Mice were decapitated without anaesthesia. Acute 250 μm thick coronal striatal brain slices (bregma, +1.54 to +0.62 mm) were cut on a vibratome and allowed to recover for at least 1 hr at room temperature in oxygenated artificial cerebrospinal fluid (ASCF, in mM): NaCl 125, KCl 2.5, $NaHCO_3$ 26, $CaCl_2$ 2.4, $MgSO_4$ 1.3, KH_2PO_4 0.3, glucose 10, HEPES 5; pH 7.3-7.4, 290-295 mOsm.

FFN511 loading and destaining. FFN511 (10 μM in ACSF) was loaded into presynaptic terminals by a 30 min incubation at room temperature. The dye bound to extracellular tissue was removed by a 30 min incubation in ADVASEP-7 (CyDex, Overland Park, KS; 100 μM in ACSF) *(6)*. The slice was then placed in a recording chamber and superfused (1ml/min) with ACSF. Slices were allowed to rest for at least 10 minutes in the chamber before imaging. For stimulation-dependent dopamine terminal destaining, stimuli at 1, 4 or 20 Hz (300 μs x 1 mA) were applied to the striatum locally by an Iso- Flex stimulus isolator triggered by a Master-8 pulse generator (AMPI, Jerusalem, Israel) using bipolar electrodes. To minimize the variation in the depolarization of release sites, we used a stimulation protocol applying 150% of the

maximal stimulation intensity determined by cyclic voltammetry. All experiments were performed at room temperature, except for (+)-amphetamine sulphate (AMPH, 20 μM) induced destaining experiments, which were performed at 36 ºC.

Imaging and data analysis. Striatal terminals were visualized using a Zeiss LSM 510 NLO multiphoton laser scanning confocal microscope with a Titanium-sapphire laser (excitation 760 nm/emission 480-520 nm) equipped with a 63 X 0.9 NA water immersion ultraviolet objective (Zeiss). Images were captured in 8-bit, 73 x 73 μm regions of interest at 512 x 512 pixel resolution and acquired at 27-second intervals using Zeiss LSM 510 software. To compensate for z-axis shift, a z-series of 5 images, separated by 1 μm in the z-plane, was obtained for each period. Some images were acquired at 60-second intervals with a z-series of 12 images. Images in each z-series were aligned and condensed with maximum transparency. The time projection was analyzed for changes in puncta fluorescence using Image J (Wayne Rosband, National Institutes of Health, Rockville, MD) and custom-written software in IDL (Research Systems, Boulder, CO) *(7)*. The striatal region of interest (ROI) where fluorescent puncta were analyzed was within 300 μm of the stimulation bipolar electrodes. Fluorescent puncta 0.3 – 1.5 μm in diameter were identified. The criteria for including puncta were: 1) spherical shape, 2) fluorescence that is two standard deviations above the background, and 3) stimulation dependent destaining. The program aligned puncta in the x, y, and z plane by shifting each image in 3 dimensions based on the location of the peak of their cross correlograms with the first z-series. Images showing projections of maximal z-axis intensity were made of each stack and the intensity of FFN511 fluorescence for each punctum was measured over the time interval. To correct for minor changes in

background fluorescence (due to minor tissue bleaching), the background fluorescence of each image (<10%) was subtracted from the fluorescence intensity of individual puncta. The results were then normalized by the maximal fluorescence intensity of that punctum just before unloading. The halftime decay of intensity during destaining ($t_{1/2}$) was determined graphically. The fractional release parameter f, was calculated from ln (F1/F2)/ ΔAP *(8)*, where F1 and F2 are the fluorescent intensities at t1 and t2, respectively and ΔAP is the number of action potentials delivered during that period.

Imaging FM1-43 with FFN511. Mouse corticostriatal slices were loaded with 10 μM FM 1-43 by incubation with the dye for 10 min in regular ACSF followed by 10 min in 40 mM KCl ACSF also containing FM 1-43. The slices were allowed to recover for 15 min in ACSF and they were then incubated with 5 μM FFN511 for 30 min. ADVASEP-7, at a concentration of 100 μM, was applied for 30 min to remove any non-specifically bound dye.

Slices loaded with FM 1-43 and FFN511 were imaged by two-photon microscopy (Leica DM6000) at an excitation wavelength of 810 nm. FM 1-43 fluorescence was detected at 570-650 nm, while FFN511 was detected at 450-510 nm. Under these conditions, the FM 1-43 and the FFN511 fluorescent signals are lower than what is obtained at their optimal excitation and emission ranges, but can be simultaneously acquired in both channels with no significant crossover. Single Z-section images from slices belonging to four different mice of similar age were obtained using the LASAF software.

Imaging FFN511 with GFP. FFN511 was excited at 760 nm, while TH-GFP was excited at 910 nm. Although FFN 511 and GFP have similar emission profiles (emission maximum ~475 nm for FFN511 and 510 nm for GFP in slices), the excitation

wavelengths are sufficiently different to allow selective imaging of each probe.

8. Cyclic voltammetry (CV). Cylinder carbon fiber electrodes of 5 μm diameter and 30 to 100 μm length were placed into the dorsal striatum. For CV, a triangular voltage wave (-400 to +900 mV at 280 V/s versus Ag/AgCl) was applied to the electrode every 100 ms. Current was recorded with an Axopatch 200B amplifier (Axon Instrument, Foster City, CA), with a low-pass Bessel Filter setting at 5 kHz, digitized at 20 kHz (ITC-18 board, Instrutech Corporation, Great Neck, New York). Triangular wave generation and data acquisition were controlled by a PC computer running a locally written IGOR program (E. Mosharov, Columbia University; WaveMetrics, Lake Oswego, OR). Striatal slices were electrically stimulated every 2 minutes with a single pulse stimulation by an Iso-Flex stimulus isolator triggered by a Master-8 pulse generator (A.M.P.I., Jerusalem, Israel) using a bipolar stimulating electrode placed at a ~100 μm distance from the recording electrode. Background-subtracted cyclic voltammograms served to identify the released substance. The DA oxidation current was converted to concentration based upon a calibration of 5 μM DA in ACSF after the experiment.

II. SUPPLEMENTAL FIGURES AND LEGENDS

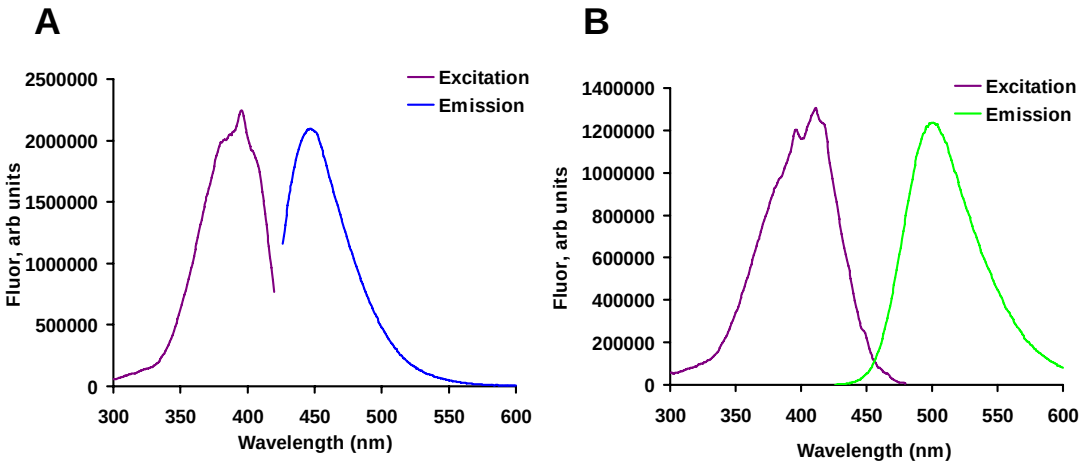

Fig. S1. FFN511 fluorescent excitation and emission spectra. **(A)** chloroform and **(B)** 100 mM sodium phosphate pH 7 buffer.

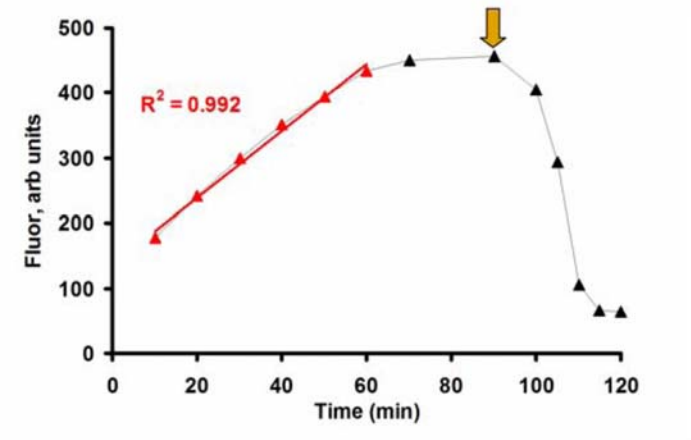

Fig. S2. Accumulation of FFN511 (350 nM) measured by epifluorescence microscopy of individual chromaffin cells, was linear from 10-60 min. The labeling was abolished by the lipophilic weak base, chloroquine (100 µM, arrow).

	Quantal size (# molecules)	Imax (pA)	$t_{1/2}$ (msec)	#events/cell	n cells recorded	%feet
FFN511	342,000 ± 35,000	15.0 ± 3.3	5.5 ± 1.0	35 ± 7	14	27
Control	291,000 ± 47,000	12.5 ± 1.4	4.9 ± 0.5	28± 3	30	25

Fig. S3. Average of the median values of quantal parameters from individual mouse chromaffin cells ± SEM. No parameters were significantly different by ANOVA, including additional parameters (e.g., slope) not shown.

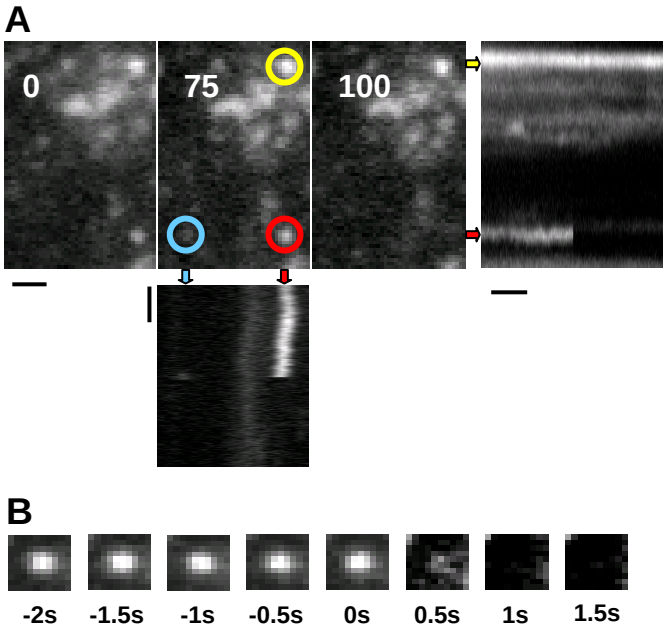

Fig. S4. (A) Cultured rat chromaffin cells were incubated with 7μM FFN511 for 10 min, and secretion was then stimulated with 90 mM K^+ starting at 60 s. Frames from the video at 0, 75 and 100 s are shown: in the second panel, a vesicle that does not fuse is circled in yellow, and one that fuses is shown in red. The blue circle indicates a vesicle that originally was not present and then either fused or moved away from the surface. The images are displayed as time series with the vesicles indicated by the colored arrows. Time scale bars are 30 sec; spatial scale bar is 1 μm. **(B)** A critique of TIRFM exocytosis experiments is that if the vesicle disappears as it moves away from the membrane, it could be mistakenly considered to have fused. We examined whether a vesicle could be caught "during the act" of exocytosis, when intermediate destaining could be observed. In this example of a single vesicle acquired as in (A), the fluorescence diffuses at 500 ms, which is thought to be evidence for exocytosis and is inconsistent with the vesicle moving away from the focal plane, which would not show expansion of the fluorescent area.

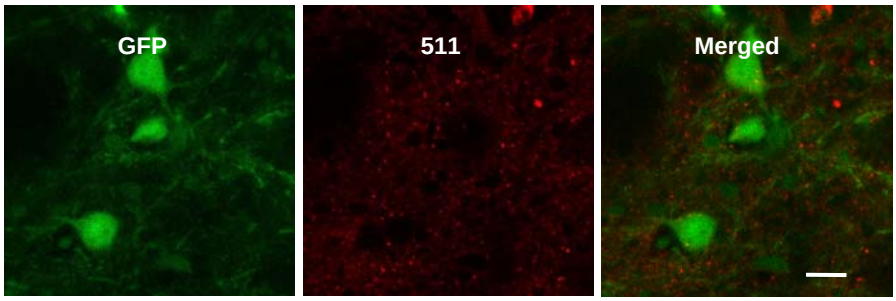

Fig. S5. FFN511 does not label GABAergic neurons and their neurites in the striatal brain slice. **(A)** Shown in green are the EGFP-labeled GABAergic striatopallidal neurons. The BAC-D2R-EGFP mice (bacterial artificial chromosome-transgenic mice that express GFP under the control of the dopamine D2 receptor promoter) were obtained from Gensat. **(B)** FFN511 labeling is shown in red. **(C)** Overlap of overall pattern of FFN511 with EGFP. FFN511 was excited at 760 nm, while EGFP was excited at 910 nm. Scale bar: 10 μm. Movie S2 shows 3-dimensional projection of this double label.

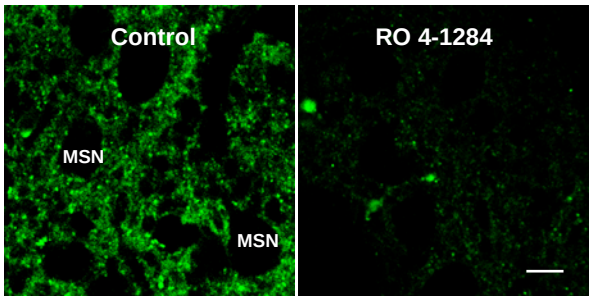

Fig. S6. FFN511 labeling was strongly inhibited by VMAT inhibitor, Ro 4-1284 (20 μM). Scale bar: 10 μm.

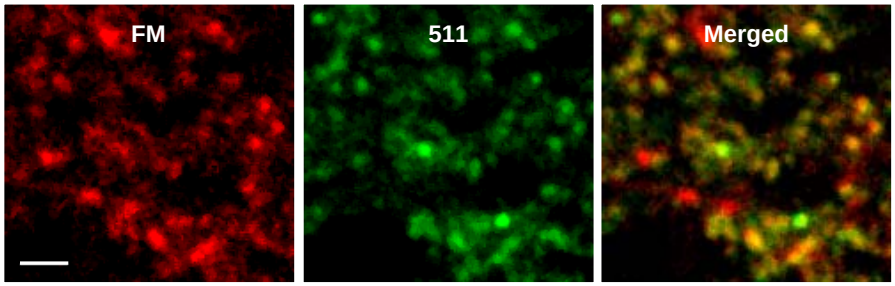

Fig. S7. Colocalization of FM 1-43 (red) and FFN511 (green) labeled terminals. Mouse corticostriatal slices were sequentially loaded with 10 µM FM 1-43 and 5 µM FFN511 and simultaneously visualized. A representative image from four independent experiments depicts extensive colocalization of FFN511 and FM 1-43 labeled terminals. Scale bar: 4 µm.

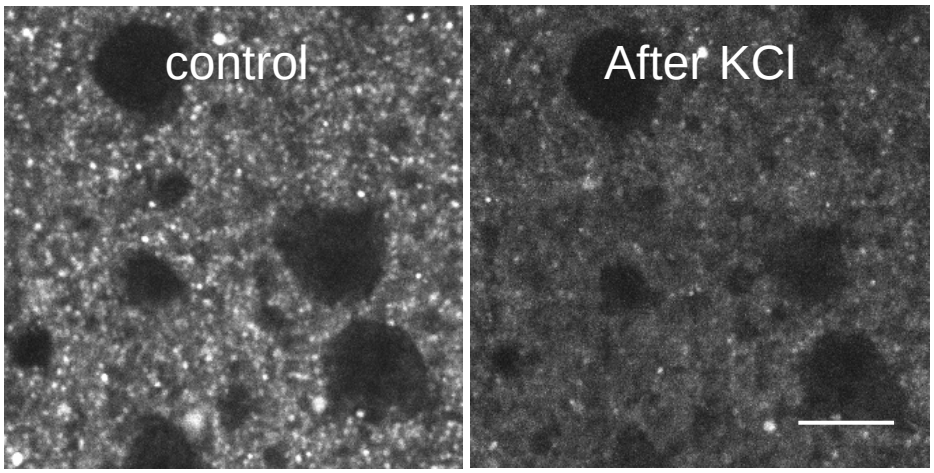

Fig. S8. Destaining of FFN511 labeling by high KCl. FFN 511 labeling is destained within 2 min application of 70 mM KCl ACSF. Scale bar: 10µm.

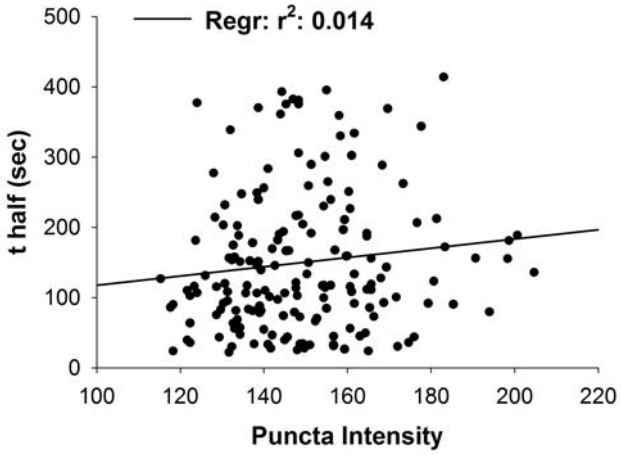

Fig. S9. Example of relationship between initial fluorescent intensity and terminal destaining. The $t_{1/2}$ of terminal destaining (y) versus initial fluorescent (x) from 1 slice at 20 Hz is fit by linear regression, y=51.39+0.66x. The coefficient r^2 is 0.014, suggesting that differences in the activity of dopamine terminals are unrelated to synaptic vesicle FFN accumulation. The analysis was performed in at least 3 slices at each frequency, and in no case was a relationship between initial fluorescent intensity and terminal destaining observed.

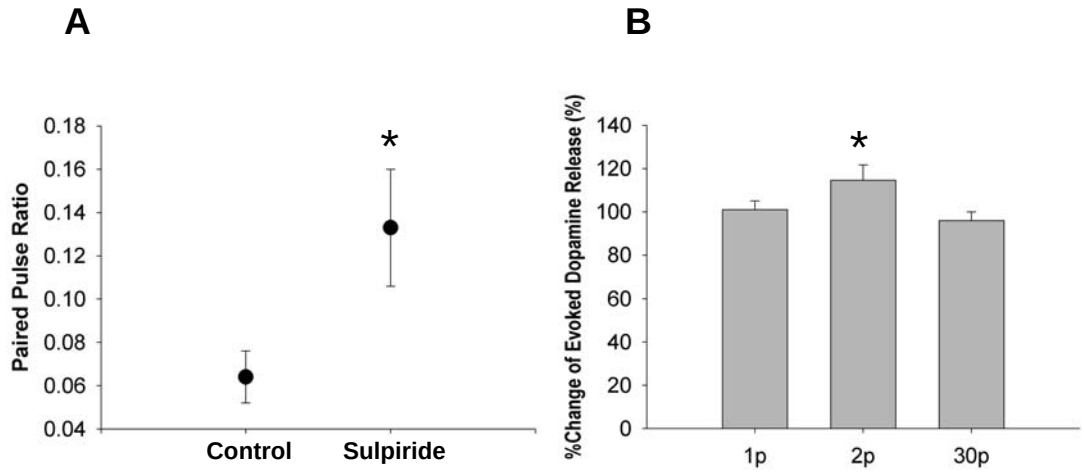

Fig. S10. Effect of sulpiride on evoked dopamine release. **(A)** Effect of sulpiride on paired pulse ratio. Sulpiride (10 μM, 20 min) increased release from the second pulse at 20 Hz (2 single pulses at an interval of 0.05 sec, paired pulse ratio is 0.133± 0.027 with sulpiride compared to 0.064± 0.012 as control, n=9, $p < 0.05$, t test), indicating D2R is effective at 20Hz. **(B)** Changes of evoked dopamine release after application of sulpiride. Sulpiride had no effect on dopamine release elicited by a single pulse (101 ± 4% of control, n=7, $p>0.05$), indicating no endogenous D2R tone in the slices. It slightly enhanced dopamine release elicited by 2 pulses at 20 Hz (114± 7%, n=6, $p < 0.05$), but it had no effect on evoked dopamine release elicited by 30 pulses at 20 Hz (96 ± 4%, n=7, $p > 0.05$). One way ANOVA (Dunnett) test.

III. Supplemental Table 1

$[Ca^{2+}]$	$t_{1/2}$ (sec)	*f*
0 mM	>5000	<0.01%
0.5 mM	258	0.067%
2.4 mM	210	0.082%
10 mM	184	0.094%

Table S1. Dependence of fractional FFN511 release per stimulus (*f*) on extracellular Ca^{2+} levels in slices stimulated at 4 Hz. Between three to five slices with a total of 205-503 puncta were measured per group.

IV. Movie Legends

Movie S1 Video micrograph from TIRF microscopy of FFN511 destaining during LDCV exocytosis from a chromaffin cell.

Movie S2 Video micrograph of a 3-dimensional projection of FFN511 label and EGFP labeled striatopallidal medium spiny neurons.

Movie S3 Video micrograph from 2-photon microscopy of FFN511 destaining during exocytosis in a striatal brain slice preparation.

V. SUPPORTING REFERENCES

1. E. V. Mosharov, L. W. Gong, B. Khanna, D. Sulzer, M. Lindau, *J Neurosci* **23**, 5835-5845 (2003).
2. E. V. Mosharov, D. Sulzer, *Nat Meth* **2**, 651-658 (2005).
3. D. Bruns, R. Jahn, *Nature* **377**, 62-65 (1995).
4. J. P. Finn, R. H. Edwards, *J Biol Chem* **272,** 16301-16307 (1997).
5. J. A. Steyer, H. Horstmann, W. Almers, *Nature* **388**, 474-478 (1997).
6. A. R. Kay *et al., Neuron* **24**, 8098-17 (1999).
7. S. S. Zakharenko *et al., Nat Neurosci* **4**, 711-717 (2001).
8. J. S. Isaacson, B. Hille, *Neuron* **18**, 143-152 (1997).